

Simplified methods of assessing the impact of grid frequency dynamics upon generating plants

Nuclear Electric

April 29, 1996

1 The problem

The frequency of the national electricity grid is affected by fluctuations in supply and demand, and so continually “judders” in an essentially unpredictable fashion around 50 Hz. At present such perturbations do not seemingly affect Nuclear Electric as most of their plant is run at more or less constant load, but they would like to be able to offer the national grid a mode of operation in which they “followed” the grid frequency: i.e., as the frequency rose above or fell below 50 Hz, the plant’s output would be adjusted so as to tend to restore the frequency to 50 Hz. The aim is to maintain grid frequency within 0.2 Hz of its notional value. Such a mode of operation, however, would cause a certain amount of damage to plant components owing to the consequent continual changes in temperature and pressure within them.

Nuclear Electric currently have complex computational models of how plants will behave under these conditions, which allows them to compute plant data (e.g., reactor temperatures) from given grid frequency data. One approach to damage assessment would require several years’-worth of real grid data to be fed into this model and the corresponding damage computed (via “cycle distributions” created by their damage experts). The results of this analysis would demonstrate one of three possibilities: the damage may be acceptable under all reasonable operating conditions; or it may be acceptable except in the case of an exceptional abrupt change in grid frequency (caused by power transmission line failure, or another power station suddenly going off-line, for instance), in which case some kind of backup supply (e.g., gas boilers) would be required; or it may simply be unacceptable.

However, their current model runs in approximately real time, making it inappropriate for such a large amount of data: our problem was to suggest alternative approaches. Specifically, we were asked the following questions:

- Can component damage be reliably estimated directly from cycle distributions of grid frequency? i.e., are there maps from frequency cycle distributions to plant parameter cycle distributions?
- Can a simple model of plant dynamics be used to assess the potential for such maps?
- What methods can be used to select representative samples of grid frequency behaviour? What weightings should be applied to the selections?
- Is it possible to construct a “cycle transform” (Fourier transform) which will capture the essential features of grid frequency and which can then be inverted to generate simulated frequency transients?

We did not consider this last question, other than to say “probably not”.

We were supplied with data of the actual grid frequency measurements for the evening of 29/7/95, and the corresponding plant responses (obtained using Nuclear Electric’s current computational model). A simplified nonlinear mathematical model of the plant was also provided.

Two main approaches were considered: statistical prediction (see section 2) and analytical modelling via a reduction of the simplified plant model (see section 3).

2 Statistics

(i) Cycles

Damage potential is currently assessed at Nuclear Electric using a pre-written code to calculate a 'cycle histogram'. This was run at the Study Group (see figure 1). Some thought was given to the possibility of relating the resulting cycle spectrum in a crude way to the power spectrum, although no specific suggestions were made.

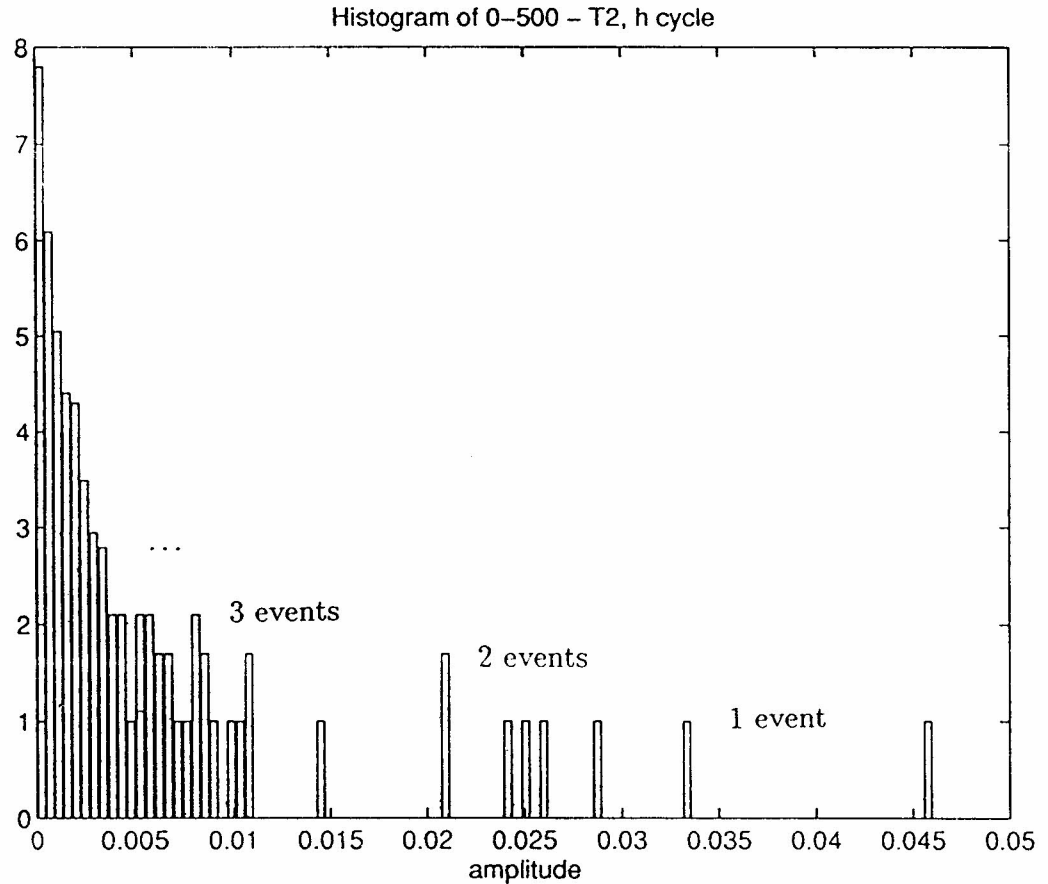


Figure 1: Histogram of the amplitudes of so-called 'H'-cycles for the supplied data (log-linear).

(ii) Power spectra

The power spectrum of the raw grid frequency data is shown in figure 2. It has a long tail. On the other hand, figure 3 is the corresponding power spectrum of the inlet gas temperature (computed from the supplied plant data). There is a sharp cut-off at the noise floor, suggestive that the plant acts as a linear filter on the grid frequency. We come back to this below.

(iii) Phase portraits

The degree of linearity can be gauged to some extent by plotting phase portraits of the model outputs. In figure 4 we show a number of these, representing plots relating grid frequency ω , circulator gas outlet temperature T_1 , channel gas outlet temperature T_2 , reheater steam exit temperature T_R , superheater steam exit temperature T_S , and reactor thermal power Q_B . It can be seen that there is, for example, good linear correlation between ω and Q_B , with some scatter. When such a

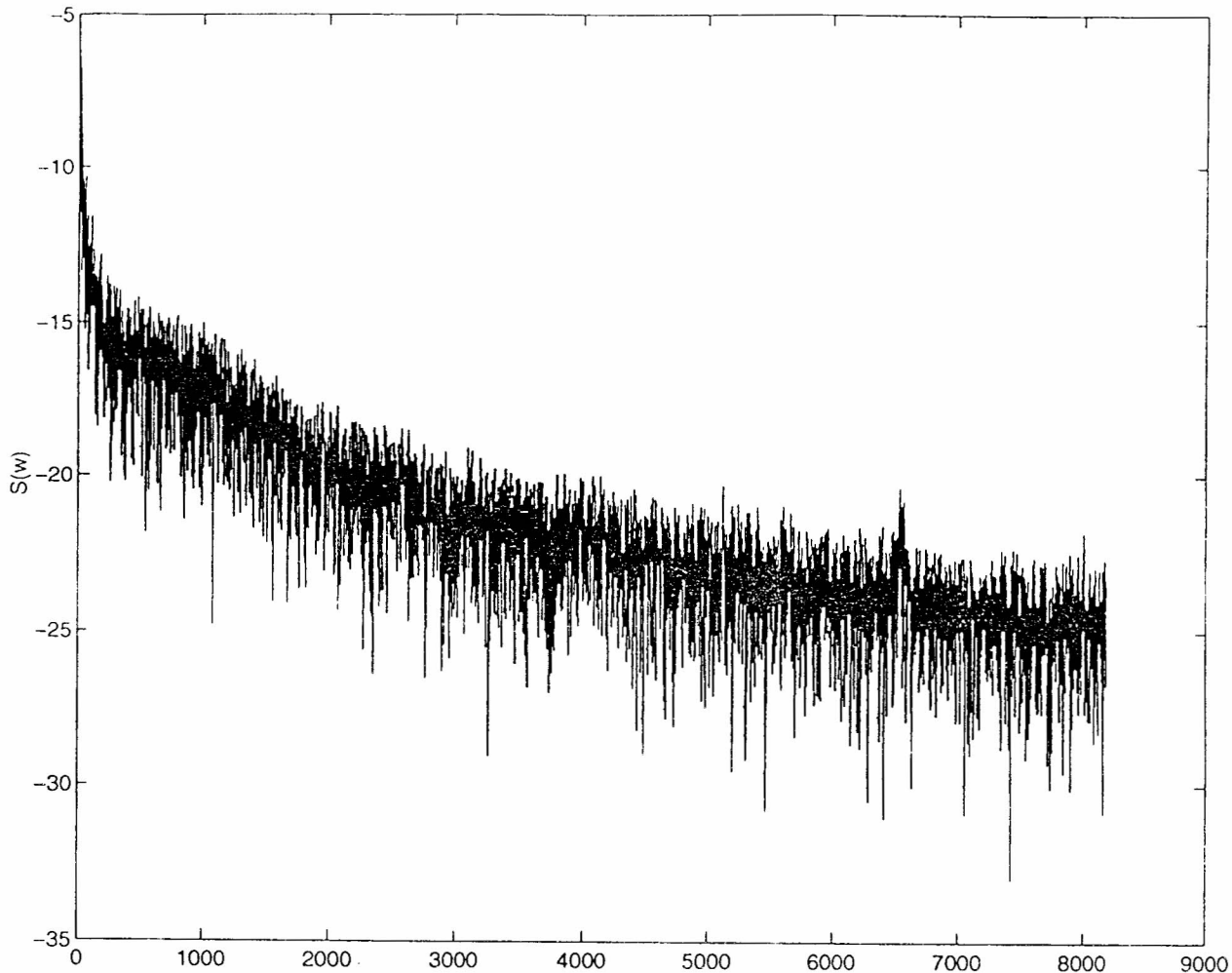


Figure 2: Power spectrum of grid frequency (natural log-linear).

plot is viewed in time (i.e., the points are added in sequence), there is apparent cycling about the linear trend, which suggests that the small scale scatter is due to nonlinear deterministic effects (as opposed to, for example, an AR model, where the sequence would appear more random in space).

(iv) Other methodologies

Lack of time, or lack of code, prevented much exploration of other techniques. Here we outline a possible scenario for future work; the small scale model described in section 3 can be used as a benchmark against which different methods of data analysis can be tested. We term this process “nonlinear modelling”. One strategy is as follows. Given the grid frequency data $\omega(t)$, we choose a suitable phase space embedding, say in \mathbb{R}^{d_E} as

$$\Omega_i = (\omega(t_i), \omega(t_i - \Delta), \dots, \omega(t_i - (d_E - 1)\Delta)),$$

where Δ is the lag and d_E is the embedding dimension. Typical choices of d_E and Δ will have $d_E\Delta \approx 200$ s (the longest response time), and $\Delta \approx 10$ s (the shortest response time), though there is flexibility in the choice. The time series $\{\omega(t_i)\}$ is now represented by the embedded trajectory $\{\Omega_i\}$. This trajectory is nonlinearly filtered by using singular value decomposition to compute the singular spectrum, $\sigma_1 \geq \sigma_2 \geq \dots \geq \sigma_{d_E}$. We filter by projecting the vectors on to the singular vectors with $\sigma_i > \delta$, where δ typically represents the noise floor. As a result, we obtain a filtered trajectory $\{\Omega_i^f\}$, where each Ω_i^f is the sum of k multiples of the k retained singular vectors. A typical value might be $k = 6$, for example.

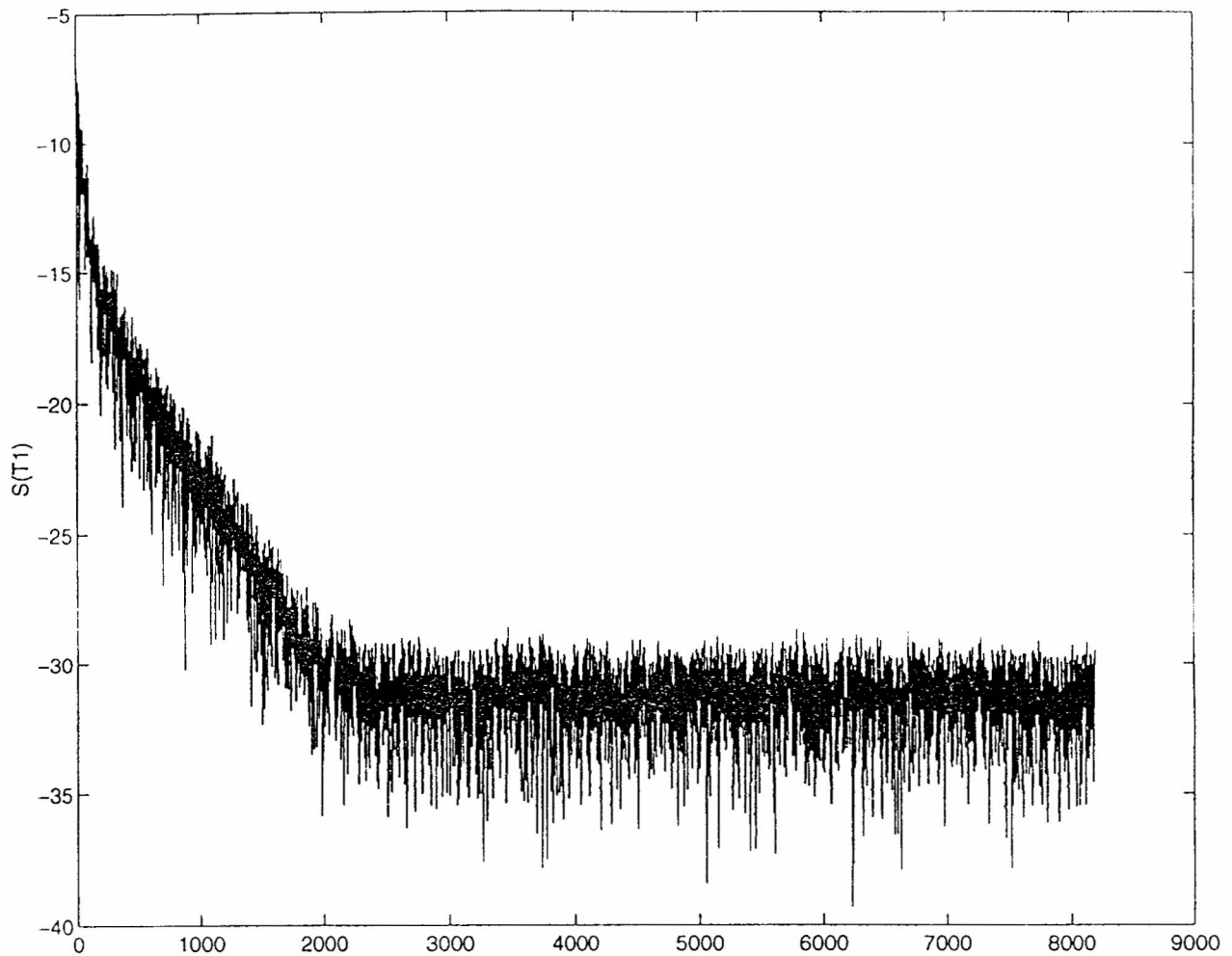


Figure 3: Power spectrum of inlet gas temperature corresponding to figure 2 (see section 3.1.1)

Finally, we build a nonlinear model by seeking a map $F : \mathbb{R}^k \rightarrow \mathbb{R}$ such that

$$F(\Omega_i^f) = T_i,$$

where T is the observable (e.g., a plant temperature) which we hope to predict. Typical examples of such nonlinear models use radial basis functions, or local (in phase space) linear predictors, to estimate F .

We may use the simple model of section 3 as a laboratory control for this method in the following way. Use the simple model to generate (given ω) the observable T . Build a nonlinear predictor (exactly as described above) to predict T from ω . Now we can estimate the value of the predictor by computing T for a different ω using the model, and comparing with the estimates from the predictor. In this way, we can gain a measure of the reliability of the nonlinear predictor for the particular data that we are considering.

3 Analytical models

3.1 The plant

Nuclear Electric provided a simplified mathematical model of a plant and its control system. This model involved a dozen or so plant parameters, including several control loops. The plant divides naturally into two sections: the reactor and boiler in one section, and the turbines and reheater in the other. Feedback comes in the form of the grid frequency, measured at the turbine shaft in

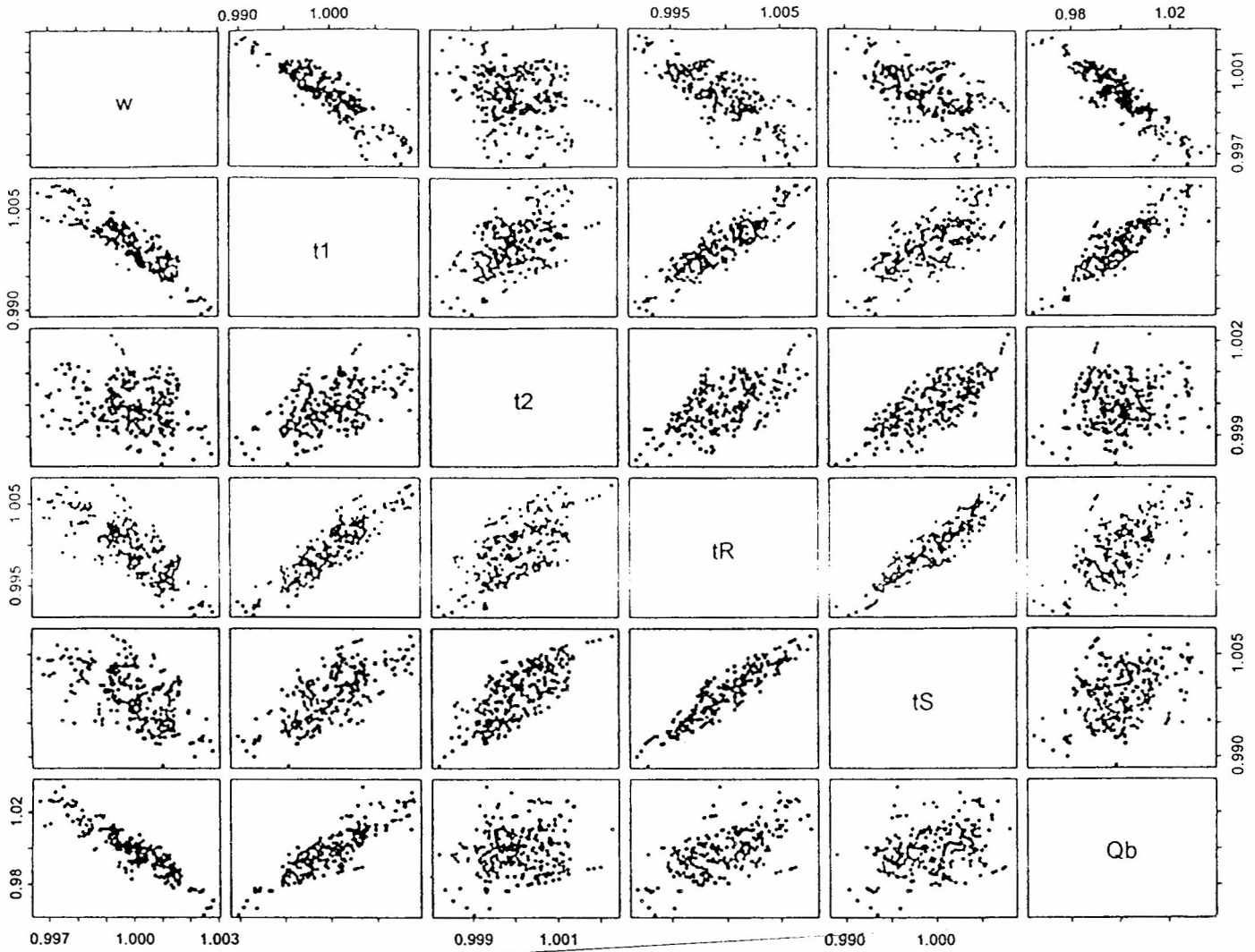


Figure 4: Phase portraits relating grid frequency and plant parameters.

the second section, which is used to control the governor regulating the boiler pressure in the first section.

It was clear that these two sections could effectively be decoupled; whilst a particular power station does have an effect on the grid frequency (via its varying electrical output at the turbines), it is only one of several such stations affecting the frequency, and so its individual effect is small. Other suppliers and the large number of consumers will be more significant, and will act so as to make the grid behave in a particular way regardless of this station's actions. The grid frequency may therefore be considered as input to the plant, unaffected by the plant's output.

We also chose to ignore the rate-limiters which control pressure and heat output in the plant; we assumed that these limiters would only be activated in extreme (or, at least, relatively unusual) circumstances.

With these considerations, the model for the boiler section of the plant becomes self-contained and linear, albeit with time-varying coefficients. We further approximated by linearizing these coefficients about their equilibrium values. Consideration of the magnitudes of the perturbations involved indicated that this *should* be a very acceptable approximation in all but extreme cases; if the grid frequency remains within the range 49.8–50.2 Hz and $\dot{\omega}$ stays within “normal” bounds (such as those in the sample data) we find ourselves within the linear regime.

With these considerations the entire model reduces to a third-order linear inhomogeneous sys-

tem:

$$\begin{pmatrix} \dot{P} \\ \dot{Q} \\ \dot{C} \end{pmatrix} = \begin{pmatrix} -A_0/\tau_B(1 + \gamma_S A_0^2) & 1/\tau_B & 0 \\ -\alpha_P p_{S_0}/\tau_F(1 + \gamma_S A_0^2) & -1/\tau_F & 1/\tau_F \\ -\alpha_P p_{S_0}/\tau_I(1 + \gamma_S A_0^2) & 0 & 0 \end{pmatrix} \begin{pmatrix} P \\ Q \\ C \end{pmatrix} + \Delta \left\{ \begin{pmatrix} P_{\text{set}}/\tau_B p_{S_0} \\ 0 \\ 0 \end{pmatrix} - \frac{2\gamma_S A_0 P_{\text{set}}}{1 + \gamma_S A_0^2} \begin{pmatrix} A_0/\tau_B p_{S_0} \\ \alpha_P/\tau_F \\ \alpha_P/\tau_I \end{pmatrix} \right\} w \quad (1)$$

where P , Q and C are perturbation plant parameters, $w = (\omega - \omega_0)/\omega_0$ (where $\omega_0 = 50$ Hz) is the normalized frequency deviation, and all other parameters are defined by the plant design (constant for a given design). We were supplied with suitable values for these parameters.

(More explicitly, P , Q and C are defined by

$$\begin{aligned} P_D &= (1 + \gamma_S A_0^2)P_{\text{set}} + p_{S_0}P, \\ Q_B &= A_0 P_{\text{set}}/p_{S_0} + Q, \\ c_I &= A_0 P_{\text{set}}/p_{S_0} + C \end{aligned}$$

in terms of the variables P_D , Q_B and c_I of Nuclear Electric's model. The constant Δ in (1) is equal to the reciprocal of the "droop": i.e., a droop of 8% means $\Delta = 12.5$.)

We write (1) in shorthand as

$$\dot{\mathbf{x}} = A\mathbf{x} + \mathbf{F}w. \quad (2)$$

Using "typical" values for the plant parameters, we calculated the eigenvalues of A as -0.0045 and $-0.0066 \pm 0.011i$. (These correspond to time constants of approx. 220 s and 150 s respectively.) We note the negativity of the real parts, as expected, for a stable control system.

These model eigenvalues give us an understanding of the inference drawn in section 2(ii) above: the matrix A acts as a low-pass filter on the power spectrum of the forcing in (2), which is proportional to w .

To check the validity of this model we used it to compute the gain in Q_B , given w . The gain at frequency Ω is defined as the modulus squared of the second entry of the column vector $(i\Omega I - A)^{-1}\mathbf{F}$. A plot of the resulting function of Ω (computed using Maple) is shown in figure 5. The corresponding gain for the supplied plant data was also calculated and appears in figure 6. The agreement in shape is excellent, both plots showing a peak at somewhat over 0.001 Hz, with a subsequent steady decay (approximately linear on these log-log scales). There is however a disagreement (even at the level of order of magnitude) between the gain values, which was accidentally overlooked by the Study Group (where the vertical scales on the two graphs were misinterpreted). This is probably due to a mismatch between the normalizations of Q_B and ω used to generate the two plots, as the plant data came from a file in which values had been renormalized. This should be further investigated, and it may be necessary to adjust the plant parameters in the model to obtain a good fit.

Further suggested work on this model includes solving (2) subject to forcing $w = W\theta(t)$, where W is a constant and θ is the Heaviside step function. This could model a sudden rise or fall in the grid frequency, caused by some drastic change in demand or supply, where W is a measure of the size of the change. Damage could be calculated analytically in this case, and a comparison with the output of the larger computational model would reveal the limits of the linear approximation.

It is hoped that this reduced model will prove effective enough to use on the "everyday" grid data. It is certainly extremely cheap computationally, and so could be run effectively on huge amounts of data. The existing large computational model could be used to fill in the gaps where the grid frequency data is unusual in various ways and in which the reduced model's validity is called into question. This combination of models should allow damage analysis, on a large enough range of data, to be carried out in reasonable time.

3.2 The grid frequency

On a short time scale the grid behaviour is dominated by changes in demand tempered by the rotational inertia of all the turbines and generators (as well as electric motors, at least in principle)

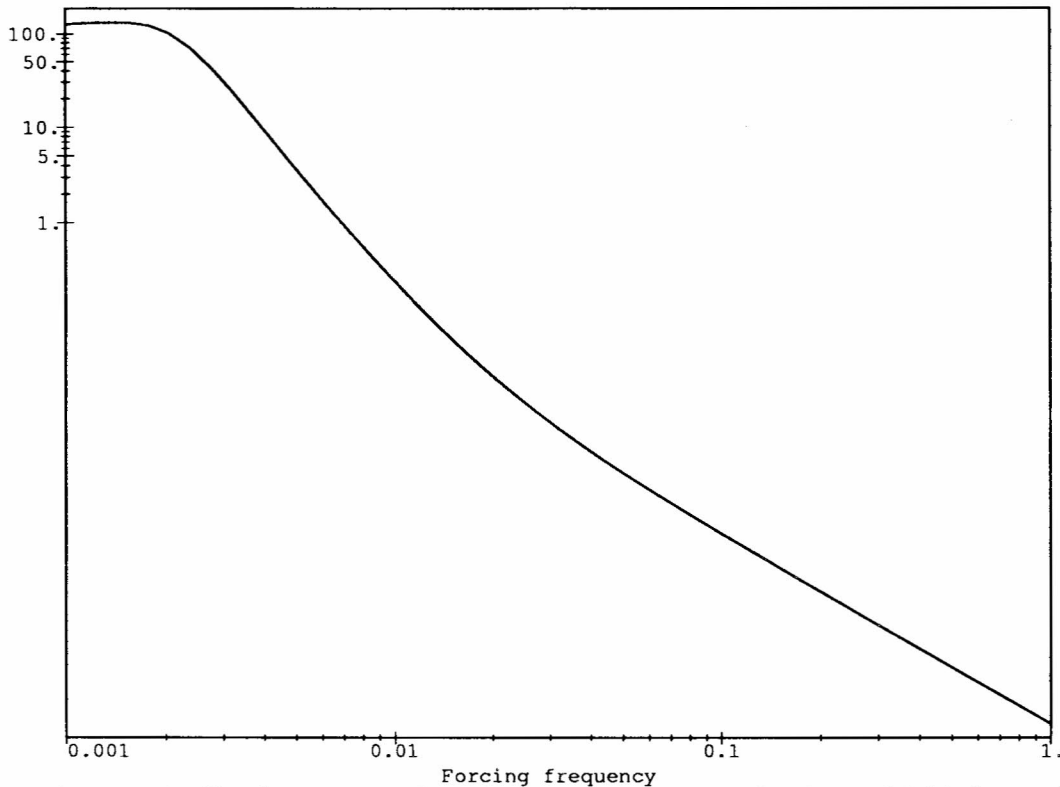


Figure 5: Predicted gain in Q_B for unit grid perturbation under the model (1) (log-log).

connected to the grid. The appropriate equation, in linearized form, is

$$E_S - \tau_I \dot{w} = E_D \quad (3)$$

where E_S represents the generated power (as delivered to the generator rotors) and E_D is the demand. The term $\tau_I \dot{w}$ represents kinetic (rotational) energy being transformed to electric power or vice versa — this term is linearized here, as the grid frequency is close to constant. If E_S and E_D are also scaled appropriately, the constant τ_I may be interpreted as a time scale: the time it would take for the demand to totally drain the rotational energy of all the generators in the absence of any generated power. In fact we shall let E_S and E_D be the normalized deviations from an equilibrium; so $E_S = E_D = 0$ at a postulated equilibrium, and they would drop to -1 if all power generation ceased.

We may, somewhat arbitrarily, estimate $\tau_I \approx 8$ s.

We model the demand E_D as a Brownian motion. This may not be too unreasonable if the demand is thought of as a large number of stochastically independent small consumers of power being switched on and off at random times. However this model only makes sense on relatively short time scales, as Brownian motion is almost surely unbounded whereas E_D is clearly bounded.

In practice the generated power E_S is not constant, but is constantly regulated in an effort to keep $w \approx 0$. We model this via the forced relaxation equation

$$\tau_S \dot{E}_S + E_S = -\Gamma w. \quad (4)$$

Here τ_S is a time constant characteristic of the control systems of those generating plants participating in frequency regulation: it is the time-scale over which those plants respond to an abrupt change in grid frequency. A value of $\tau_S \approx 10$ s may be considered typical. Γ expresses the relative strength of this control mechanism: a change in w equal to $1/\Gamma$ (the “droop”) will result in a 100% change in generated power. A droop of 4% has been suggested, corresponding to $\Gamma = 25$.

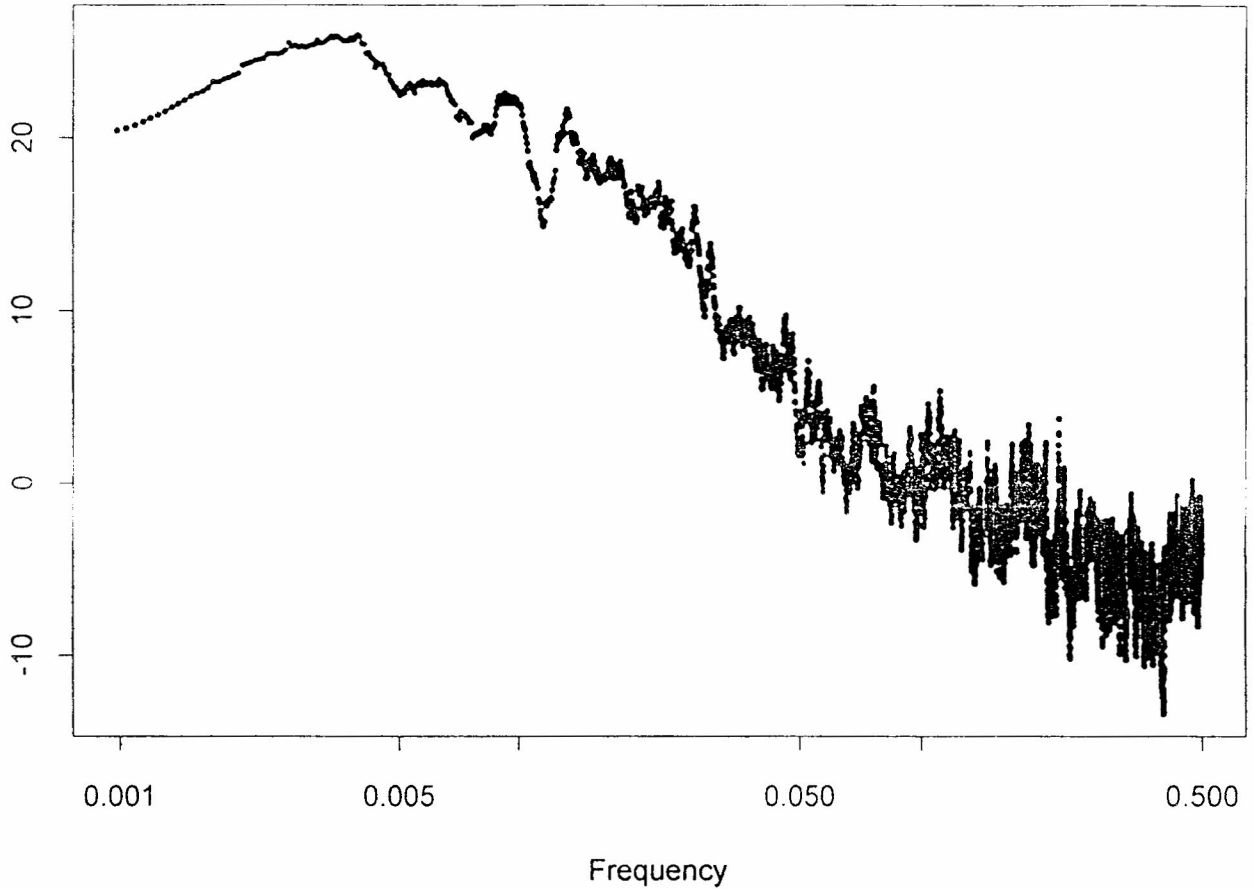


Figure 6: Gain in Q_B for unit grid perturbation calculated from the supplied plant data (log-log). The values on the vertical axis give the natural logarithm of the gain.

However, only a fraction of stations follow the grid at any time, so perhaps a proportion $\Gamma \approx 4$ is more appropriate.

If we eliminate E_S from the two equations (3) and (4) the equation

$$\tau_S \tau_I \ddot{w} + \tau_I \dot{w} + \Gamma w = -(E_D + \tau_S \dot{E}_D) \quad (5)$$

results. This has to be interpreted with some caution, as the time derivative of Brownian motion — white noise — only exists in a generalized sense.

We need a bit of notation.

If y is a stationary stochastic process with finite variance on the real line, its autocorrelation

$$R_y(t') = E[y(t)y(t+t')]$$

is a function of t' alone, and its Fourier transform

$$S_y(\varphi) = \int_{-\infty}^{\infty} R_y(t') e^{i\varphi t'} dt'$$

is called the *spectral density* or the *power spectrum* of the process. The process is called ergodic if $S_y(\varphi) = |\hat{y}(\varphi)|^2$ for almost every sample path y (where \hat{y} is the Fourier transform of y).

In general we think of white noise as a stationary process whose autocorrelation is a delta function, and whose spectral density is therefore a constant function. Its integral, Brownian motion, is not stationary, but if it were, the theory would make its power spectrum equal to a

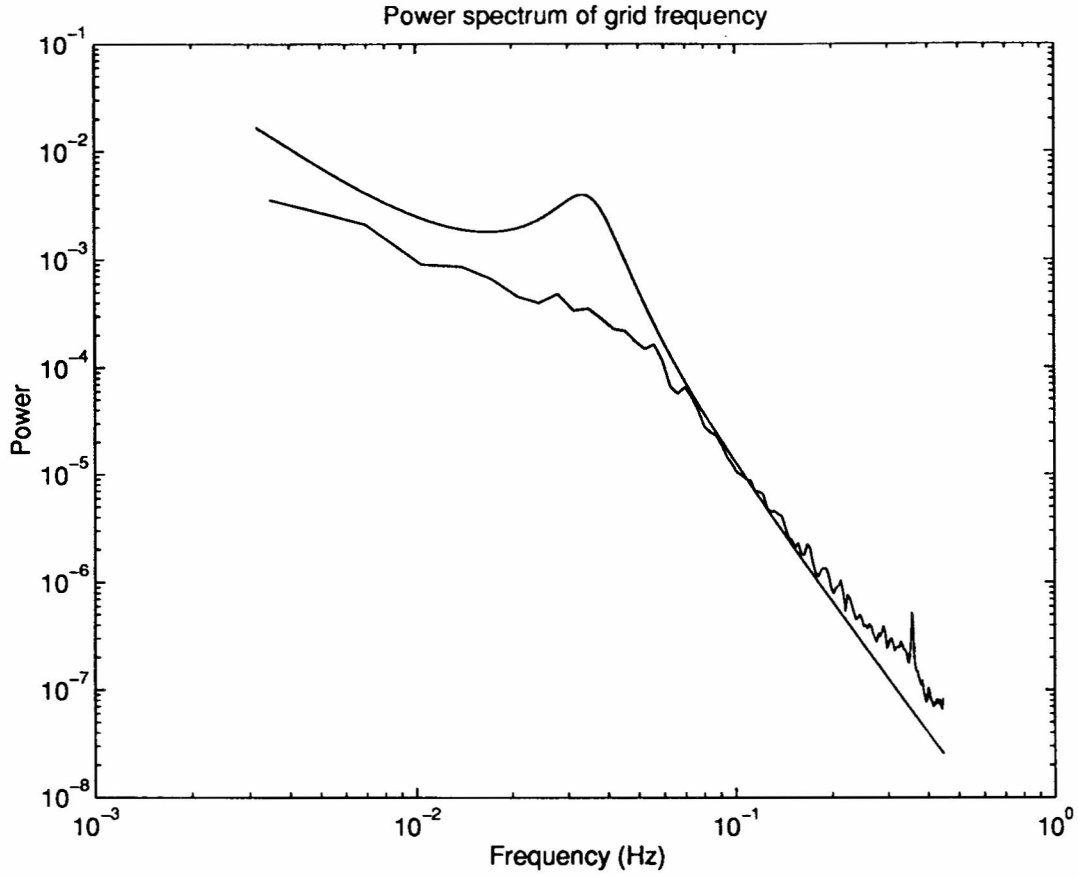


Figure 7: Actual power spectrum estimated from data on the evening of 29/7/95 (jagged curve) and from the model (smooth curve).

constant times $1/\varphi^2$. In fact Brownian motion does have stationary increments, so this argument can be made rigorous with a little more work — see, e.g., Doob (*Stochastic processes* pp. 434–436, Wiley, 1953).

Formally taking Fourier transforms on both sides of (5) we get

$$(-\tau_S \tau_I \varphi^2 - i\tau_I \varphi + \Gamma)\hat{w}(\varphi) = -(1 - i\tau_S \varphi)\hat{E}_D(\varphi)$$

or, taking absolute values and squaring,

$$|\hat{w}(\varphi)|^2 = \frac{1 + (\tau_S \varphi)^2}{(\Gamma - \tau_S \tau_I \varphi^2)^2 + (\tau_I \varphi)^2} |\hat{E}_D(\varphi)|^2.$$

With the above assumption on the power spectrum of E_D , we would get a power spectrum of w proportional to

$$\frac{1 + (\tau_S \varphi)^2}{((\Gamma - \tau_S \tau_I \varphi^2)^2 + (\tau_I \varphi)^2) \varphi^2}. \quad (6)$$

In figure 7 this power spectrum is computed and overlaid on the spectrum estimated from the observed data. Apart from the model's resonance near 0.03 Hz, the fit looks fairly reasonable. An explanation for the absence of an observed resonance in the data might be that different grid followers operate with different values of τ_S , which might help to obscure any resonance.

3.3 A typical day

How might we select representative samples of grid frequency: i.e., can we produce some “typical days”? The jagged curve in figure 7 shows that the power spectrum of the grid frequency (for the night in question) divides fairly cleanly into two regions: up to around a frequency $\varphi = 0.05$ Hz, a region approximately proportional to $\varphi^{-0.6}$, and beyond that a region proportional to φ^{-2} . The work in section 3.2 shows that the second region results substantially from Brownian motion; the main qualitative difference between different days of the year is therefore likely to be in the first region. We might expect different gradients (instead of -0.6) and different amplitudes depending on the season and the time of day. The Study Group’s suggestion is to compute the power spectra from the grid data for a large number of days and smooth off (or even cut off completely) the φ^{-2} regions. From these, extreme examples should be taken, as well as suitably averaged selections, for each significant time of day, week and year. The selected spectra could then be converted back to “representative” time series for ω .

Contributors

Robert Hunt, Andrew Fowler, Harald Hanche-Olsen, Tim Drye, Isla Gilmour, Pat McSharry, Colin Please, Stefan Llewellyn-Smith.